

The low mass companion of HIP 45314 (HR 3672)*

C. Adam^{1†}, R. Neuhauser^{1‡}, M. Mugrauer¹, J. G. Schmidt¹, T. O. B. Schmidt¹

¹*Astrophysikalisches Institut und Universitäts-Sternwarte, Schillergässchen 2-3, D-07745 Jena, Germany*

ABSTRACT

We report the discovery of a very low-mass companion to HIP 45314 (HR 3672) located about $2.7''$ north-west of HR 3672 A. With four years of epoch difference between the two observations obtained with the Very Large Telescope we can reject by more than 4σ that B would be a non-moving background object unrelated to A. HR 3672 A is a B 7-8 main sequence star with an age of 140 ± 80 Myr and from the magnitude difference between HR 3672 A and B and the 2MASS magnitudes, we can estimate the magnitude of HR 3672 B ($K_s = 12.42 \pm 0.28$ mag) and then, for age and distance of the primary star, using models, its luminosity and mass ($0.2 - 0.5 M_\odot$). We present a reanalysis of the probable membership of HR 3672 A to the Platais 9 cluster, and introduce a new method for astrometric calibration of data without dedicated calibration images. In the deepest available image (co-add of all epochs) no additional companion candidates within $13''$ were detected down to $0.03 M_\odot$.

Key words: Astrometry - binaries: visual - stars: individual: HR 3672 - open clusters and associations: individual: Platais 9.

1 INTRODUCTION

It is still not clear, whether massive stars form preferentially by accretion of material through a circumstellar disk or by coagulation of lower mass stars in a multiple system. Maybe, both ways of formation are possible, then it is still unknown, how often each of the two channels is chosen by nature. High and intermediate mass stars very often are multiple (Zinnecker & Yorke 2007) with a binary fraction of 70 to 90 % (Pfalzner & Olczak 2007; Ostrov 2002). Yet, for many high and intermediate mass stars, no deep and sensitive multiplicity survey has been done. In particular, only few of these stars have been observed so far by AO imagers, which can find very faint, maybe sub-stellar, companions also at a separation range (roughly 0.1 to few arc sec, i.e. long orbital periods), which is not reachable for spectroscopic surveys (short periods). This object is part of our study of multiplicity of B-type stars in European Southern Observatory (ESO) archival Adaptive Optics (AO) imaging data. With this project we can study the statistical aspects of multiplicity among intermediate mass stars, analyse their distribution with respect to mass and separation and obtain constraints on the underlying processes in their formation. Here we show first results of

our project.

The star HIP 45314 (also called HR 3672, distance 161.3 ± 6.7 pc at $\alpha(J2000) = 09^h14^m08^s.2$ and $\delta(J2000) = -44^\circ08'45''$ according to van Leeuwen (2007), $V = 5.839$ mag according to Simbad) is located in the Vela constellation. Platais et al. (1998) identified HR 3672 as a possible member of the open cluster HIP 45189 (no probability of membership given) with an age of ~ 100 Myr (for details, see Secion 4.3). The spectral type of HR 3672 is B6IV according to Simbad, but as reported in the literature by different authors (and summarized e.g. by Skiff 2010), mainly yielded spectral types between B4V and B7V (see Sec. 4.2 and Sec. 4.3). The star is also suspected to be variable with an amplitude in V of 0.05 mag (Kukarkin et al. 1981).

We also use this object exemplary to introduce an alternative method for the astrometric calibration (self-calibration of pixel scale and detector orientation) of data by using the science images instead of extra recorded calibration binaries or clusters.

The order of this paper is as follows. In Sec. 2 the observations and data reduction are presented. A detailed description of the self-calibration for astrometry is given in Sec. 3. Furthermore we show the result of the common proper-motion pair analysis in Sec. 4.1 and the age and mass estimation for HR 3672 A and B in Sec. 4.3 and Sec. 4.4, respectively. The limits on detection of further companions are explained in Sec. 4.5 and the conclusions are collected in Sec. 5.

* Based on data products from observations made with ESO Telescopes at the La Silla Paranal Observatory under programme IDs 074.D-0180(A) and 080.D-0348(A).

† E-mail: christian.adam.1@uni-jena.de

‡ E-mail: rne@astro.uni-jena.de

Table 1. Observations log

Epoch	Optics & Filter	<i>DIT</i> [s]	<i>NDIT</i>	<i>N</i>	<i>FW</i>
2004-12-16	S27/K _S + ND _{Short}	0.3454	149	9	90
2008-02-15	S27/K _S + ND _{Short}	1.0	50	9	101

Note. With detector integration time (*DIT*), the number of detector integrations per frame (*NDIT*), the total number of frames (*N*), and the full width (*FW*) at half maximum in milli arc seconds are given.

2 OBSERVATIONS AND DATA REDUCTION

The data presented here are part of an archival search for unknown companions of B-type stars within 1 kpc. We reduced all publicly available data of B-type stars taken with the Adaptive Optics camera NACO (for Nasmyth Adaptive optics system with the COude near-infrared imager and spectrograph, Rousset et al. 2003; Lenzen et al. 2003) located in a VLT/UT4 (Yepun) Nasmyth focus.

The data-set of HR 3672 consists of two epochs, one observed in 2004¹ with a total integration time of 7.7 min, and one from 2008² with a total integration time of 7.5 min (for details see Table 1). In addition calibration data, i.e. darks with same exposure time as science frames, and lampflats with same filter as science frames, were taken from archive. Master-dark and flat field images for each epoch were created with *esorex*³, which is part of ESO’s Common Pipeline Library⁴ (CPL). After removal of bad pixel with *IDL/sigma_filter* (Landsman 1993) from each science image, darks and flats were applied using ESO *ECLIPSE/jitter*⁵. Finally we co-added all images with *esorex*, using the provided shift+add procedure. The fully reduced image, taken in December 2004, is shown in Figure 1.

To obtain the position of HR 3672 A and its companion candidate (henceforth, B) for all epochs we used MIDAS center/gauss (Warmels 1992) on the reduced images. Neither A nor B are saturated.

In order to determine the spectral type of HR 3672 we also used a well exposed, so far unpublished spectrum of the star, which was obtained by the International Ultraviolet Explorer (IUE) on 1993 Feb 13th. The spectrum was taken with IUE’s short-wavelength spectrograph (1150-1980 Å) and its prime camera (SWP) in the high resolution mode ($\Delta\lambda \sim 0.2 \text{ \AA}$, and an average dispersion of about $0.04 \text{ \AA}/\text{pixel}$), using the large aperture (slot width $10'' \times 20''$). The total integration time of the spectrum is 434.865 s.

3 ASTROMETRIC CALIBRATION

Usually astrometric calibrations are obtained from binaries or clusters with known separations and position angles,

¹ Public data from the ESO data archive, taken in ESO program 074.D-0180(A)

² Public data from the ESO data archive, taken in ESO program 080.D-0348(A)

³ <http://www.eso.org/sci/software/cpl/esorex>

⁴ <http://www.eso.org/sci/software/cpl>

⁵ ESO C Library for an Image Processing Software Environment.

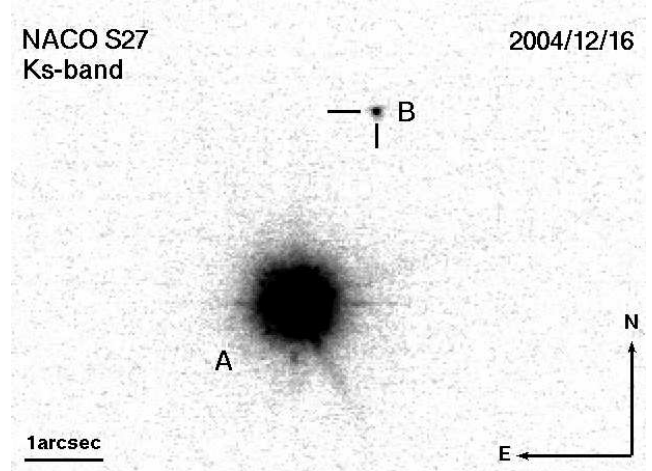


Figure 1. VLT-NACO S27 image of HR 3672 and its faint companion candidate ($\Delta K_s = 6.4 \text{ mag}$) taken on 2004-12-16 in Ks-band. The total integration time is 7.7 min. Since the companion candidate is found to be co-moving (Sec. 4.1), we can call it B.

which are observed with the same setup in the same night. In some cases neither calibration binaries nor clusters were observed for a data-set or it is very time-consuming to find adequate calibrations. In these cases it is still possible to achieve an acceptable astrometric calibration using a technique which we call self-calibration. A first limited usage was performed in Schmidt et al. (2008) and Neuhäuser et al. (2010). In this section we now give a detailed description of the approach to this method using the example of HR 3672.

The basic idea of the self-calibration is to obtain the pixel scale (*PS*) and the rotation angle (θ) of the detector from the science images itself using the non-shifted and non-added reduced images. Two information’s are needed for the calculation:

- (1) position of objects on the detector x_i, y_i in pixel-units
- (2) *RA* and *DEC* coordinates of the telescope pointing, stored in the FITS-header keywords *CRVAL1* and *CRVAL2*

For object detection we first used *SExtractor* (Bertin & Arnouts 1996) to get a raw position of the objects on the detector. We then passed the results to *IDL/starfinder* (Diolaiti et al. 2000) to obtain a more accurate object detection. From the resulting set of pixel positions $\{x_i, y_i\}_k$ ($k = 1 \dots N$, where *N* is the total number of frames) we then calculate the shift of an object on the detector between each frame by

$$\Delta x \stackrel{i \neq j}{=} x_i - x_j, \quad \Delta y \stackrel{i \neq j}{=} y_i - y_j.$$

The result is a new set of variables $\{\Delta x, \Delta y\}_{m=1}^n$ in which the number of sets *n* is given by

$$n = \frac{N(N-1)}{2}.$$

Hence, for HR 3672 ($N = 9$ for both epochs as number of frames, i.e. of different telescope offsets) we get $n = 36$ pairs of values, assuming that at least one object, namely the brightest, was detected in each frame. The set of coordinate values $\{\Delta RA, \Delta DEC\}_{m=1}^n$, which gives the shift of the telescope pointing, is calculated by

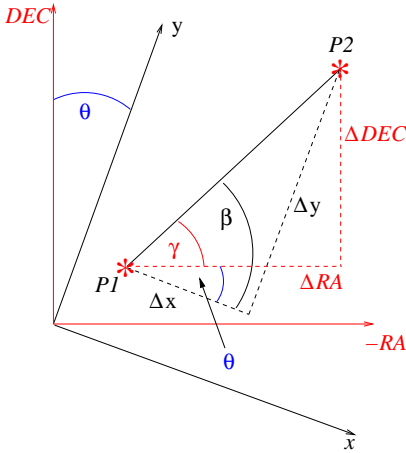


Figure 2. Schematic diagram for the rotation angle of the detector θ . The points $P1$ and $P2$ indicate the position of the object in two frames. The difference between the frames in detector coordinates is shown by Δx , Δy and their corresponding angle β , as well as the difference in world coordinates (ΔRA , ΔDEC) with the angle γ . The rotation angle θ is calculated as difference of β and γ ; this angle gives the detector orientation.

$$\Delta RA \stackrel{i \neq j}{=} -(RA_i - RA_j) \cos(\overline{DEC})$$

and

$$\Delta DEC \stackrel{i \neq j}{=} DEC_i - DEC_j,$$

where \overline{DEC} is the average of DEC_i and DEC_j , and $\cos(\overline{DEC})$ is the cosine-correction between the 3D world coordinate system (WCS) and the 2D image coordinate system. From this we then can derive the separation $D_{Det.}$ on the detector and $D_{WC.}$, the separation in world coordinates, by taking the root of the sum of squares. The pixel scale is then given by

$$PS_m = \frac{D_{WC,m}}{D_{Det.,m}} \quad \text{for } m = 1 \dots n. \quad (1)$$

For the calculation of the detector rotation angle θ we use the fact that the amount of de-rotation is given by the difference of the rotated detector, here labelled as β , against the angle of the non-rotated world coordinate system, labelled as γ . Fig. 2 shows a scheme of the de-rotation of the two coordinate systems. Hence, we get

$$\theta_m = \beta_m - \gamma_m \quad \text{for } m = 1 \dots n, \quad (2)$$

where β_m and γ_m are given by

$$\beta_m = \arctan\left(\frac{\Delta y}{\Delta x}\right), \quad \gamma_m = \arctan\left(\frac{\Delta DEC}{\Delta RA}\right).$$

From this sample of data we excluded those values by 3σ -clipping, whose deviations are $> 3\sigma$ around the mean. In Fig. 3 (upper panel) we show the result from the pixel scale calculation for December 2004 as function of the measurement number. All errors are calculated by largest error-estimation. Since this method is based on relative distances, we use the tracking-error of the VLT/UT4 (Yepun) of $0.1''^6$ for error estimation. Furthermore we calculated the weighted

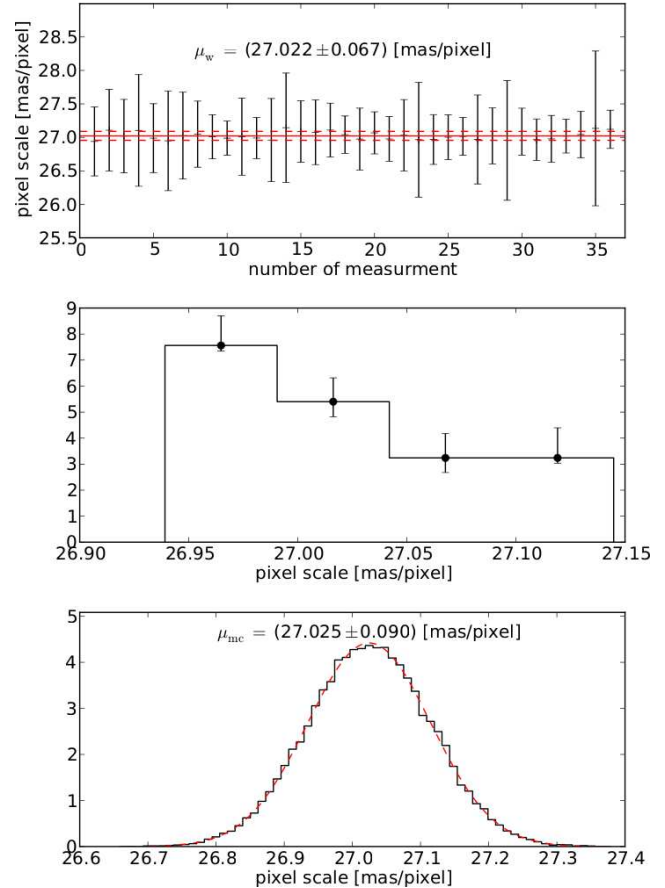


Figure 3. We show the results from the self-calibration method. In the upper panel we show the pixel scales and the weighted mean of the values (μ_w); the distribution of the data-set (middle panel), with bin-sizes calculated by Freedman-Diaconis choice (Freedman & Diaconis 1981) and errors from deviation of re-sampled data-points with 15000 iterations. The lower panel shows the histogram of the artificially increased sample with 50000 iteration steps using Monte-Carlo. The best fit for normal distributed values is indicated by the (red) dashed line, with the mean pixel scale $\mu_{mc} = 27.025 \pm 0.090$ mas/pixel.

mean of the data-set (full and dashed lines in Fig. 3 upper panel) and show the distribution of the data (middle panel). Because the number of data is a low-number statistic we artificially increased the sample with a Monte-Carlo simulation (for details of principal see, e.g. Wall & Jenkins (2003)) with 50000 iterations. We assumed that the underlying distribution is a Gaussian. To test the significance of the null hypothesis we used a Shapiro-Wilk test for normality (Shapiro & Wilk 1965). The results show that the null hypothesis can be accepted at a significance level of $> 95\%$. With this assumption we generated normal distributed values including the errors from our data-set, which gave us the final result (mean and standard deviation) for the pixel scale PS and the detector rotation angle θ shown in Tab. 2.

To test our self-calibration technique we use six data-points published in Neuhäuser et al. (2008) calibrated with the binary HIP 73357, all with NACO S13. We re-reduced the science data and used our method to calculate pixel scale and detector orientation for each epoch. The results are shown in Tab. 3. The comparison of the two methods

⁶ RMS of tracking-error for all VLT/UTs according to ESO

Table 3. Comparison of our new self-calibration for GQ Lup with normal astrometric calibration with a binary

GQ Lup Epoch	(Neuhäuser et al. 2008)		this work, self-calibration	
	PS [mas/pixel]	θ [°]	PS [mas/pixel]	θ [°]
2005-05-27	13.240 ± 0.050	0.21 ± 0.33	13.221 ± 0.059	0.23 ± 0.24
2005-08-08	13.250 ± 0.052	0.35 ± 0.34	13.279 ± 0.056	0.14 ± 0.24
2006-02-22	13.238 ± 0.053	0.18 ± 0.35	13.205 ± 0.063	0.12 ± 0.28
2006-05-20	13.233 ± 0.055	0.39 ± 0.36	13.172 ± 0.049	0.22 ± 0.23
2006-07-16	13.236 ± 0.055	0.43 ± 0.36	13.241 ± 0.059	0.06 ± 0.22
2007-02-19	13.240 ± 0.059	0.34 ± 0.38	13.304 ± 0.128	0.06 ± 0.55

Table 2. Results of self-calibration for HR 3672

Epoch	Optics	PS [mas/pixel]	θ [°]
2004-12-16	S27	27.025 ± 0.090	0.033 ± 0.191
2008-02-15	S27	27.200 ± 0.104	0.017 ± 0.218

Note. We list the pixel scale (PS) and the rotation angle (θ) of the detector and their uncertainties for the used epochs.

shows that the results for the pixel scale and detector orientation are consistent within the 1σ errors. The errors on the detector orientation for our new self-calibration method are in most cases smaller than in Neuhäuser et al. (2008), but possible NACO field distortions could not be considered in our self-calibration. The fact that the pixel scale values on the GQ Lup data obtained from self-calibration scatter more than in Neuhäuser et al. (2008) points to field distortions. Such distortions could be larger in S27 than in S13. But overall, our self-calibration should be consistent within the errors.

The presented method can be used in principal for all imaging techniques which use a dither method, but the accuracy of the results is strongly dependent on the tracking accuracy of the telescope, i.e. a ten times larger tracking-error for example would result in a ten times larger error in the rotation angle. Therefore this self-calibration should only be considered as rough estimation for data-sets without astrometric calibrators.

4 RESULTS

4.1 Astrometry

With the results of the self-calibration (see above) we get the separation ρ on the detector and the true, corrected position angle (PA) for HR 3672 A and its companion candidate, listed in Tab. 4. The companion candidate is located $\approx 2.73''$ north-west of HR 3672 A (PA $\approx 336.7^\circ$). To check for common proper motion and orbital motion we use the astrometric data from Simbad: Proper motion $\mu_\alpha \cos(\delta) = -24.77 \pm 0.27$ mas/yr and $\mu_\delta = 13.10 \pm 0.20$ mas/yr, distance $\pi = 6.20 \pm 0.27$ mas (or 161.3 ± 6.7 pc), from van Leeuwen (2007). Applying the Smith-Eichhorn (Smith & Eichhorn 1996, equation 21 therein) correction (to obtain the more reliable expectation value), we derive $\pi = 6.26 \pm 0.27$ mas or 159.7 ± 6.6 pc, respectively. The calculations presented here are done using this corrected parallax, but the results are almost identical for the Hipparcos parallax without Smith-Eichhorn correction.

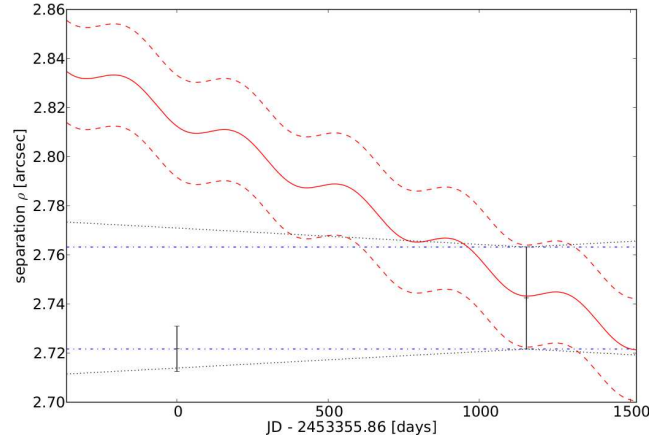


Figure 4. Plot of separation versus time-difference (in days) between observations for data listed in Tab. 4. Shown are the expected orbital motion for a circular edge-on orbit (dotted line); the background-hypothesis (full line), i.e. the expected change in separation assuming that the faint companion candidate is a non-moving background object, with errors including parallax and proper motion errors. The data point is inconsistent with the background hypothesis by a significance of 4σ and consistent with common proper motion (within dashed lines).

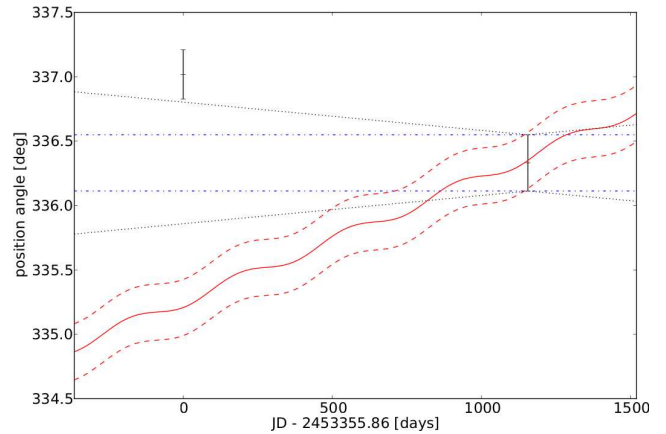


Figure 5. Plot of position angle versus time-difference (in days) between observations for data listed in Tab. 4. Shown are the expected orbital motion for a circular pole-on orbit (dotted line); the background-hypothesis (full line), i.e. the expected change in position angle assuming that the faint companion candidate is a non-moving background object, with errors including parallax and proper motion errors. The data point is inconsistent with the background hypothesis by a significance of 6σ . The PA values are deviant by about 2σ , possibly due to orbital motion.

Table 4. Astrometry of HR 3672 A and its companion candidate

Epoch	ρ ["]	ρ_{bg} ["]	s_{bg} [σ]
2004-12-16	2.722 ± 0.009	2.812 ± 0.021	4.0
2008-02-15	2.742 ± 0.021	-	-
Epoch	PA [$^\circ$]	PA _{bg} [$^\circ$]	s_{bg} [σ]
2004-12-16	337.018 ± 0.192	335.208 ± 0.218	6.2
2008-02-15	336.331 ± 0.218	-	-

Note. Shown are the separation ρ and the position angle PA (measured from North over East) of the companion candidate (B) with respect to HR 3672 A, the expected separation (ρ_{bg}) and position angle (PA_{bg}) if B would be a non-moving background object, and probability (s_{bg} , in Gaussian σ) at which the hypothesis of a non-moving background object can be rejected.

In the Figs. 4 and 5 we show the data from Tab. 4. We can reject the hypothesis that the companion candidate to HR 3672 A is a non-moving background object by 4σ & 6σ for the given epoch difference of 4 yr, and so we regard HR 3672 A and B as common proper motion pair. At the distance of HR 3672 the projected physical separation of HR 3672 A+B would be 438 ± 25 AU. We also show the expected maximum orbital motion for a circular orbit of HR 3672 B around A, being $\lesssim 2.4$ mas/yr change in separation for an edge-on orbit (Fig. 4) and $\lesssim 0.08^\circ$ /yr change in PA for a pole-on orbit (Fig. 5). The coverage of the orbit (period 4400 yr for circular orbit) from the two epochs is $< 0.1\%$ so that we only can propose that HR 3672 B is orbiting around A. It is still possible that the two objects are uncorrelated, showing a similar 2D motion on sky. The PA values are deviant by about 2σ , possibly due to orbital motion.

4.2 Spectral Classification of HR 3672 A

To determine the mass of the companion, we need to know well the age and spectral type of the primary. Depending on literature, the given spectral type of HR 3672 varies from B4V to B7V, see Buscombe (1969); Thackeray et al. (1973); Walker (1973); Cucchiari et al. (1977); Houk (1978). In contrast to the other authors Hiltner et al. (1969) gives B6IV, i.e. lists HR 3672 as non-main sequence star. This is not sufficient precise, so that we try to determine its spectral type with more precision.

In the spectral range, covered by the IUE observations (1150-1980 Å), the slope of the spectral continuum is expected to flatten from early to late type B stars, while the prominence of the Ly- α -line (at 1216 Å) should strengthen towards later spectral types. Hence, these characteristics are well usable for spectral classification.

We compared the flux-calibrated IUE spectrum⁷ of HR 3672 with template spectra from Pickles (1998). Thereby, we re-sampled the UV spectrum of HR 3672 to match the resolution of the comparison spectra. The re-sampled IUE spectrum of HR 3672 together with the spectral templates of early to late type B stars are shown in Fig. 6.

⁷ obtained from the IUE archive <http://sdc.laefl.inta.es/ines/>

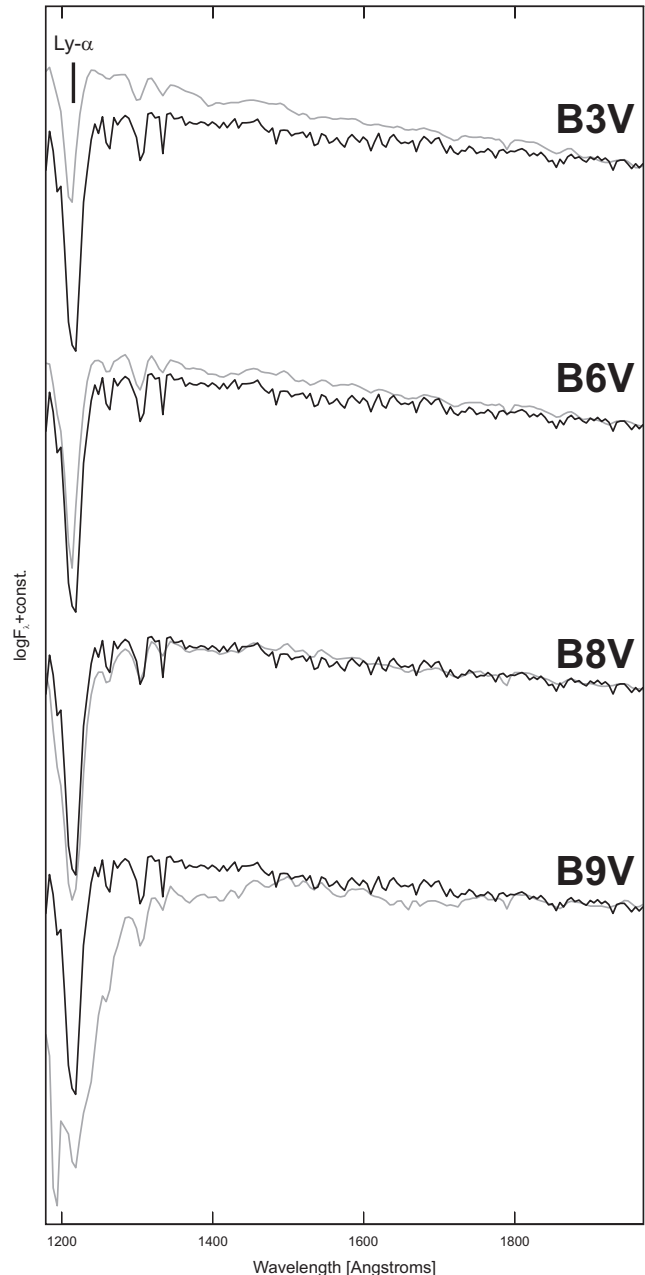


Figure 6. The IUE spectrum of HR 3672 (black) compared to template spectra (grey) of early to late type B stars from Pickles (1998). The spectrum of HR 3672 is most consistent with a late type B dwarf with a spectral type between B7V to B8V.

We find that the slope of the spectrum of HR 3672 is clearly flatter than the ones of the comparison spectra earlier than B6V, while it is steeper than the slope of the B9V template spectrum. Furthermore, the Ly- α -line in the spectrum of HR 3672 is more prominent than the Ly- α -lines in the spectral templates earlier than B6V, while it is clearly weaker than the one of the B9V comparison spectrum. Hence, both the shape of the continuum, as well as the strength of the detected Ly- α -line are consistent with a spectral type between B7V and B8V and we will exclude B6IV from our further investigations.

Table 5. Photometry data from Vizier for HR3672 A

Bmag	Vmag	Ref.
-	5.83±0.03	Hog & von der Heide (1976)
5.731±0.003	5.842±0.003	Kharchenko (2001)
5.69±0.01	5.82±0.01	Lasker et al. (2008)
-	5.847±0.011	Mermilliod (2006)
-	5.846±0.002	Hauck & Mermilliod (1998)
-	5.844±0.017	Guarinos (1995)
5.740±0.004	5.850±0.003	Myers et al. (2001)
5.687±0.014	5.818±0.009	Ammons et al. (2006)
-	5.845±0.006	Slawson et al. (1992)

4.3 Mass and Age of HR 3672 A

The B-type star HR 3672 (HIP 45314) has different published V-band and B-band magnitudes that are formally not consistent within their errors in each band. HR 3672 might be a variable star (Samus et al. 2009), thus, we take the median value with standard deviation from the V-band magnitudes published in the last decade (Kharchenko 2001; Lasker et al. 2008; Mermilliod 2006; Myers et al. 2001; Ammons et al. 2006, see Tab. 5), yielding $V = 5.842 \pm 0.015$ mag. With the same procedure we obtain for the B-band magnitude $B = 5.721 \pm 0.027$ mag. The JHK magnitudes are measured by 2MASS ($J = 6.061 \pm 0.019$ mag, $H = 6.154 \pm 0.033$ mag, $K_s = 6.134 \pm 0.027$ mag), see Cutri et al. (2003). Using B and V magnitude we derive an intrinsic colour of $(B - V) = -0.121 \pm 0.042$ mag, consistent with a B6-7 main-sequence star (Kenyon & Hartmann 1995).

We will calculate the extinction A_V , effective temperatures T and bolometric corrections B.C. (as well as masses and ages) for B7V and B8V in the following. With the BVJHK colours and effective temperatures listed in Bessell et al. (1998) we obtain $T_{\text{eff}} = 13000^{+1000}_{-1100}$ K and $BC_V = -0.85 \pm 0.20$ mag leading to $A_V = 0.05 \pm 0.04$ mag for a B7V star (using the absorption models by Cardelli et al. 1989; Rieke & Lebofsky 1985; Savage & Mathis 1979). For a B8V star we obtain $T_{\text{eff}} = 11900^{+1100}_{-1400}$ K, $BC_V = -0.66 \pm 0.24$ mag and $A_V = 0.00 \pm 0.04$ mag.

With magnitudes, A_V values, distances and bolometric corrections we obtain $L_{\text{bol}} = 212 \pm 65 L_{\odot}$ and $L_{\text{bol}} = 170 \pm 67 L_{\odot}$ for B7V and B8V, respectively. With effective temperatures and luminosities, we now can estimate age and mass of HR 3672 using the models for stellar evolution from Bertelli et al. (1994); Claret (2004) and Schaller et al. (1992). To account for possible uncertainties in the determination of the spectral type and different model temperatures we allow a relative error of one spectral type for the effective temperatures and search for the closest isochrones and mass-tracks in the model (within the error box from temperature and luminosity) and interpolate linearly between neighbouring data points (note, the model from Schaller et al. 1992 has 1 100 data points, whereas the model from Claret 2004 has 61 000 data points).

First, we calculate the masses and ages for a B7V star. For solar metallicity we obtain $3.75 M_{\odot}$, $3.98 M_{\odot}$ and $4.00 M_{\odot}$ (for the models from Bertelli et al. 1994; Claret 2004 and Schaller et al. 1992, respectively), i.e. with

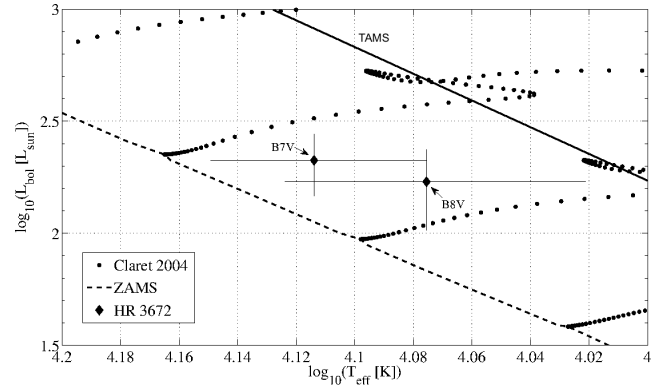


Figure 7. Mass tracks in the stellar evolution models of Claret (2004). The error-bars for the luminosity are calculated from the errors of the magnitude, parallax, extinction and bolometric correction and the error for the temperatures is assumed to be one spectral type. We also show the zero age main sequence (ZAMS, dotted line) and the termination age main sequence (TAMS, full line).

median and standard deviation from all models we obtain $3.91 \pm 0.14 M_{\odot}$. With the same models we obtain the ages 79 Myr, 27 Myr and 59 Myr, and a median age of 59 ± 37 Myr, respectively. For a B8V star we get masses of $3.45 M_{\odot}$, $3.16 M_{\odot}$ and $3.00 M_{\odot}$ (with same order of the models), hence $3.20 \pm 0.23 M_{\odot}$ and ages of 158 Myr, 225 Myr and 223 Myr (for the models from Bertelli et al. 1994; Claret 2004 and Schaller et al. 1992, respectively), hence 223 ± 38 Myr. These values for luminosity, temperature and mass are fully consistent with $\log g = 4$ for a B7-8 main sequence star. In both cases, HR 3672 lies well on the main sequence (see Fig. 7), between ZAMS and TAMS.

HR 3672 was identified as probable member of the possible open cluster HIP 45189 by Platais et al. (1998) and is located in or near the Vela OB association. Using the radial velocity measurements, proper motions and trigonometric parallaxes we can check, whether the Platais 9 cluster according to Platais et al. (1998) with previous Hipparcos data (Perryman & ESA 1997) is still a cluster with the revised Hipparcos data (van Leeuwen 2007) and radial velocities. We have calculated the U, V and W heliocentric velocity components in the directions of the Galactic center, Galactic rotation, and north Galactic pole, respectively, with the formulation developed by Johnson & Soderblom (1987) for the members of the Platais 9, Trumpler 10 and IC 2391 cluster, as shown in Fig. 8. Note that the right-handed system is used and we applied corrections for solar motion with respect to the local standard of rest (LSR) (Dehnen & Binney 1998) and galactic rotation of the sun ($V_{\text{gal}, \odot} = 220$ km/s, see Kerr & Lynden-Bell (1986)).

Fig. 8 shows that the 5 stars of the cluster Platais 9 (including our star HR 3672), for which both proper motions from Hipparcos and radial velocity (Gontcharov 2006) are known, do cluster in all three velocities (and in location in space anyway). The stars of the cluster Trumpler 10 and IC 2391 also shown in Fig. 8 also do form a cluster in all 3 velocities, which are similar to Platais 9, but the locations in space are different. With this results from our calculations we can confirm the conclusions from Platais et al. (1998), that HR 3672 is a member of the cluster called Platais 9.

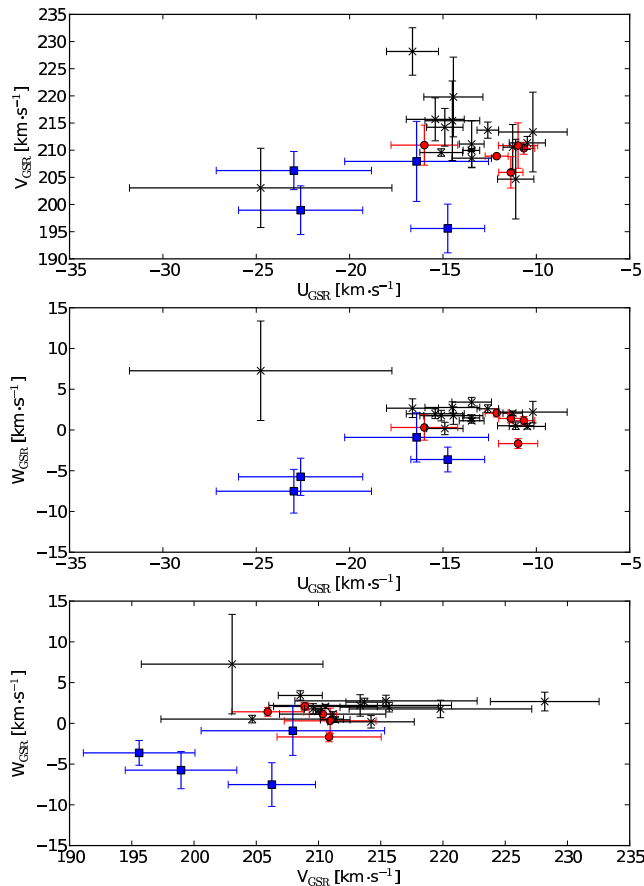


Figure 8. U, V, and W heliocentric space motions (right-handed system) with errors for the members of Platais 9 (circle), Trumpler 10 (square) and IC 2391 (asterisk) calculated from data according to Anderson & Francis (2012) (for details, see Tab. B1). The space motions are corrected for solar motion with respect to the local standard of rest (LSR) (Dehnen & Binney 1998) and galactic rotation of the Sun (Kerr & Lynden-Bell 1986). According to Platais et al. (1998), HR 3672 is a member of the possible HIP 45189 cluster. The results from our calculations show that the members of the Platais 9 cluster, including HR 3672, do cluster in UVW and space. Similar UVW results can be obtained for Trumpler 10 and IC 2391, but locations in space are different.

Using colour-magnitude-diagrams (CMD) and theoretical isochrones from Yale Rotating Evolution Code (Demarque et al. 2008) Platais et al. (1998) found an age for the cluster HIP 45189 and HR 3672 A of ~ 100 Myr, but applied no correction for reddening, i.e. the objects may be shifted to blue colours and, hence, lower ages.

HR 3672 has a non-detection in the ROSAT All-Sky Survey with an upper limit to the X-ray luminosity being $3.006 \mu\text{W}$, i.e. $\log(L_x/L_{\text{bol}}) < -6.45$ (Berghoefter et al. 1996). This ratio gives only a very high age upper limit of several Gyr (Mamajek & Hillenbrand 2008). **This consideration holds, if the X-ray emission would come from the primary. If the emission would come only from the secondary, and we assume the maximum X-Ray emission for M-type stars (see below) with $\log(L_x/L_{\text{bol}}) \sim -3$ (Fleming et al. 1993), then the upper age limit would be roughly ≈ 70 Myr according to X-ray - Age correlation by Preibisch & Feigelson**

(2005) for $0.2 - 0.4$ solar mass stars. It also turns out, that even at this young age the X-ray luminosity of HR 3672 B is too low for detection.

4.4 Mass of HR 3672 B

Since the only observable for the determination of the mass of HR 3672 B is the magnitude difference in the K-band, we calculate the absolute K-band magnitude of HR 3672 A for a B7V and B8V star, respectively, taking the absorption in the K-band A_K into account. With the absorption models by Cardelli et al. (1989); Rieke & Lebofsky (1985) and Savage & Mathis (1979) and the values for A_V (see above) we obtain $A_K = 0.006 \pm 0.005$ mag for a B7V star and $A_K = 0.000 \pm 0.005$ mag for a B8V star, respectively. Using the apparent K-band magnitude $K_s = 6.134 \pm 0.027$ mag (Cutri et al. 2003) and distance we obtain an absolute K-band magnitude of $M_K = 0.10 \pm 0.24$ mag for HR 3672 A + B together (unresolved).

With $\Delta K_s = 6.28 \pm 0.13$ mag between HR 3672 B and A, and distance, we obtain $M_{K,A} = 0.099 \pm 0.236$ mag for HR 3672 A, and $M_{K,B} = 6.38 \pm 0.48$ mag for the B-component in K-band. At 59 ± 37 Myr, for a B7V star, we derive a mass of $0.30 \pm 0.1 M_\odot$ and $0.3 \pm 0.1 M_\odot$ from evolutionary models by Baraffe et al. (1998) and Siess et al. (2000). In case of a B8V star we obtain an age of 223 ± 38 Myr and masses of $0.40 \pm 0.05 M_\odot$ and $0.4 \pm 0.1 M_\odot$ from Baraffe et al. (1998) and Siess et al. (2000), respectively. Using empirical relations by Delfosse et al. (2000) and the absolute magnitude in K-band, we derive a mass of $0.38 \pm 0.05 M_\odot$. Hence, HR 3672 B would be a low-mass stellar object of spectral type M.

4.5 Limits on further companions

For the co-added image (VLT NACO 2004+2008), no additional companion candidates were detected within $13''$. Assuming an age of ~ 60 Myr (see Sec. 4.3), sub-stellar objects would be detectable outside of $0.7''$ (or ~ 112 AU). For an age of 1 Myr, sub-stellar objects would be detectable outside of $0.2''$. Hence, HR 3672 B would be a sub-stellar object.

The determination of the dynamic range is done by measurement of the 5σ level above the background noise in the co-added image from both epochs. We compared the measured background flux from groups of 3×3 pixels with the flux of the central star HR 3672 A. In Fig. 9 we plot the flux ratio between background and HR 3672 A for the co-added images.

5 CONCLUSIONS

From the archival data of HR 3672/HIP 45314 obtained with VLT NACO with 4 yrs epoch difference, we could reject ($> 3\sigma$) the background hypothesis, that HR 3672 B is unrelated to HR 3672 A. Hence, HR 3672 A and B form a common proper motion pair. The small change in separation and the irregularity of the position angle may indicate orbital motion. No additional companions were detected within $13''$. Using unpublished IUE UV-spectra, we could narrow the spectral type of HR 3672 A down to a B7-8 main-sequence

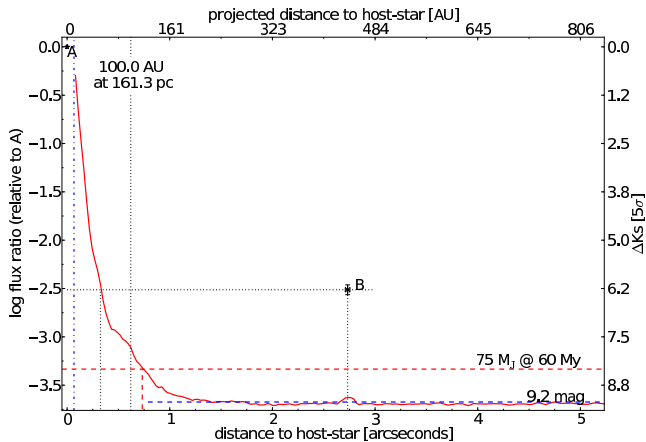


Figure 9. Dynamic range of HR 3672 for the co-added images from 2004-12-16 and 2008-02-15 in Ks-band. We plot the log flux ratio between background and HR 3672 A as function of the separation in arc-seconds. The dashed-dotted line (blue) indicates the defraction limit of the VLT/UT4 ($D = 8.2$ m) in the Ks-band ($\lambda = 2.18 \mu\text{m}$). The full (red) line shows the measured 5σ noise-level. Objects below this line cannot be detected. The background-level remains constant at $\Delta K_s = 9.2$ mag for separations outside of $1.5''$ ($0.05 M_\odot$ at 60 Myr). At 100 AU ($0.6''$ at 161.3 pc), we could detect companions with 7.7 mag difference ($0.11 M_\odot$ at 60 Myr); other companions as faint as HR 3672 B could be detected for $\geq 0.3''$ (or 48 AU). Furthermore we show the brown-dwarf limit ($75 M_J$) for 60 Myr as dashed line (red). Hence, sub-stellar objects were detectable outside of $0.7''$ (or ~ 112 AU).

star. With evolutionary models from Bertelli et al. (1994); Claret (2004) and Schaller et al. (1992), respectively, we derive a mass range of 3 to 4 M_\odot for HR 3672 A. From models we obtain ages of ~ 60 Myr for a B7V star, and ~ 220 Myr for a B8V star, respectively.

By comparison of U, V, W heliocentric space motion with surrounding cluster we can confirm HR 3672 to be a member of the cluster Platais 9 (Platais et al. 1998) with an age of about 100 Myr.

The magnitude difference between HR 3672 A and B is $\Delta K_s = 6.28 \pm 0.13$ mag, and with $K_s = 6.134 \pm 0.027$ mag (2MASS) for HR 3672 A+B, we get $K_s = 12.42 \pm 0.28$ mag for HR 3672 B. Given the magnitude difference and age of HR 3672 A of 60 to 220 Myr we derive a mass of 0.15 to 0.5 M_\odot from evolutionary models (e.g. Baraffe et al. (1998), or Siess et al. (2000)) and empirical mass-luminosity relations by Delfosse et al. (2000). Hence, HR 3672 B is a low mass star. The high uncertainties in mass of B can be decreased by taking spectra of HR 3672 B to get the physical parameters with small uncertainties.

ACKNOWLEDGEMENTS

RN, CA and TOBS wish to acknowledge Deutsche Forschungsgemeinschaft (DFG) for grant NE 515/35-1. JS wish to thank SFB for grant. This research has made use of the SIMBAD database and the VizieR catalogue access tool, operated at CDS, Strasbourg, France and archival data from the ESO, 2MASS and INES (ESA IUE Project).

REFERENCES

- Anderson, E., & Francis, C., 2012, VizieR Online Data Catalog, 5137, 0
- Ammons, S. M., Robinson, S. E., Strader, J., Laughlin, G., Fischer, D., & Wolf, A., 2006, ApJ, 638, 1004
- Banase, K., et al., 2004, Astronomical Data Analysis Software and Systems (ADASS) XIII, 314, 392
- Baraffe, I., Chabrier, G., Allard, F., & Hauschildt, P. H. 1998, A&A, 337, 403
- Berghoefner, T. W., Schmitt, J. H. M. M., & Cassinelli, J. P., 1996, A&AS, 118, 481
- Bertelli, G., Bressan, A., Chiosi, C., Fagotto, F., & Nasi, E., 1994, A&AS, 106, 275
- Bertelli, G., Nasi, E., Girardi, L., & Marigo, P., 2009, A&A, 508, 355
- Bertin, E., & Arnouts, S., 1996, A&AS, 117, 393
- Bessell, M. S., Castelli, F., & Plez, B., 1998, A&A, 333, 231
- Burrows, A., et al., 1997, ApJ, 491, 856
- Buscombe, W., 1969, MNRAS, 144, 31
- Cardelli, J. A., Clayton, G. C., & Mathis, J. S., 1989, ApJ, 345, 245
- Claret, A., 2004, A&A, 424, 919
- Claret, A., 2004, VizieR Online Data Catalog, 3424, 40919
- Chabrier, G., Baraffe, I., Allard, F., & Hauschildt, P., 2000, ApJ, 542, 464
- Cucchiaro, A., Macau-Hercot, D., Jaschek, M., & Jaschek, C., 1977, A&AS, 30, 71
- Cutri, R. M., et al., 2003, VizieR Online Data Catalog, 2246, 0
- Dehnen, W., & Binney, J. J., 1998, MNRAS, 298, 387
- Delfosse, X., Forveille, T., Ségransan, D., et al., 2000, A&A, 364, 217
- Demarque, P., Guenther, D. B., Li, L. H., Mazumdar, A., & Straka, C. W., 2008, Ap&SS, 316, 31
- Devillard, N., 2001, Astronomical Data Analysis Software and Systems X, 238, 525
- Diolaiti, E., Bendinelli, O., Bonaccini, D., Close, L. M., Currie, D. G., & Parmeggiani, G., 2000, Proc. SPIE, 4007, 879
- Freedman D., & Diaconis P., Probability theory and Related Fields, 57, 453, 1981.
- Gontcharov, G. A., 2006, Astronomy Letters, 32, 759
- Gray, D. F., 1992, Camb. Astrophys. Ser., Vol. 20,,
- Guarinos, J., 1995, VizieR Online Data Catalog, 5086, 0
- Fleming, T. A., Giampapa, M. S., Schmitt, J. H. M. M., & Bookbinder, J. A., 1993, ApJ, 410, 387
- Hauck, B., & Mermilliod, M., 1998, A&AS, 129, 431
- Hiltner, W. A., Garrison, R. F., & Schild, R. E., 1969, ApJ, 157, 313
- Hog, E., & von der Heide, J., 1976, Astronomische Abhandlungen der Hamburger Sternwarte, 9, 1
- Houk, N., 1978, Ann Arbor : Dept. of Astronomy, University of Michigan : distributed by University Microfilms International, 1978-
- Johnson, D. R. H., & Soderblom, D. R., 1987, AJ, 93, 864
- Kenyon, S. J., & Hartmann, L., 1995, ApJS, 101, 117
- Kerr, F. J., & Lynden-Bell, D., 1986, MNRAS, 221, 1023
- Kharchenko, N. V., 2001, Kinematika i Fizika Nebesnykh Tel, 17, 409
- Kharchenko, N. V., Scholz, R.-D., Piskunov, A. E., Röser, S., & Schilbach, E., 2007, Astronomische Nachrichten,

328, 889
 Kukarkin, B. V., Kholopov, P. N., Artiukhina, N. M., et al., 1981, Nachrichtenblatt der Vereinigung der Sternfreunde, 0
 Lafrenière, D., Jayawardhana, R., Janson, M., Helling, C., Witte, S., & Hauschildt, P., 2011, ApJ, 730, 42
 Landsman, W. B., 1993, Astronomical Data Analysis Software and Systems II, 52, 246
 Lasker, B. M., et al., 2008, AJ, 136, 735
 Lenzen, R., et al., 2003, Proc. SPIE, 4841, 944
 van Leeuwen, F., 2007, A&A, 474, 653
 Levato, H., Malaroda, S., Morrell, N., Solivella, G., & Grosso, M., 1996, A&AS, 118, 231
 Mamajek, E. E., & Hillenbrand, L. A., 2008, ApJ, 687, 1264
 Mermilliod, J. C., 2006, VizieR Online Data Catalog, 2168, 0
 Myers, J. R., Sande, C. B., Miller, A. C., Warren, W. H., Jr., & Tracewell, D. A., 2001, VizieR Online Data Catalog, 5109, 0
 Neuhäuser, R., Mugrauer, M., Seifahrt, A., Schmidt, T. O. B., & Vogt, N., 2008, A&A, 484, 281
 Neuhäuser, R., Schmidt, T. O. B., Hambaryan, V. V., & Vogt, N., 2010, A&A, 516, A112
 Ostrov, P. G., 2002, MNRAS, 336, 309
 Palla, F., & Stahler, S. W., 1999, ApJ, 525, 772
 Perryman, M. A. C., & ESA, 1997, ESA Special Publication, 1200,
 Pfalzner, S., & Olczak, C., 2007, A&A, 475, 875
 Pickles, A. J., 1998, PASP, 110, 863
 Pourbaix, D., Tokovinin, A. A., Batten, A. H., et al., 2004, A&A, 424, 727
 Platais, I., Kozhurina-Platais, V., & van Leeuwen, F., 1998, AJ, 116, 2423
 Preibisch, T., & Feigelson, E. D., 2005, ApJS, 160, 390
 Rieke, G. H., & Lebofsky, M. J., 1985, ApJ, 288, 618
 Rousset, G., et al., 2003, Proc. SPIE, 4839, 140
 Samus, N. N., Durlevich, O. V., & et al., 2009, VizieR Online Data Catalog, 10, 2025
 Savage, B. D., & Mathis, J. S., 1979, ARA&A, 17, 73
 Schaller, G., Schaerer, D., Meynet, G., & Maeder, A., 1992, A&AS, 96, 269
 Schmidt, T., Neuhäuser, R., & Mugrauer, M., 2008, IAU Symposium, 248, 126
 Shapiro, S. S., & Wilk, M. B., 1965, An analysis of variance test for normality (complete samples), Biometrika, 52, 3 and 4, pages 591-611
 Siess, L., Dufour, E., & Forestini, M., 2000, A&A, 358, 593
 Skiff, B. A., 2010, VizieR Online Data Catalog, 10, 2023
 Slawson, R. W., Hill, R. J., & Landstreet, J. D., 1992, ApJS, 82, 117
 Smith, H., Jr., & Eichhorn, H., 1996, MNRAS, 281, 211
 Thackeray, A. D., Tritton, S. B., & Walker, E. N., 1973, MmRAS, 77, 199
 Turon, C., Creze, M., Egret, D., et al., 1993, Bulletin d'Information du Centre de Données Stellaires, 43, 5
 Walker, E. N., 1973, The Observatory, 93, 75
 Wall, J. V., & Jenkins, C. R., 2003, Princeton Series in Astrophysics
 Warmels, R. H., 1992, Astronomical Data Analysis Software and Systems I, 25, 115
 Zinnecker, H., & Yorke, H. W., 2007, ARA&A, 45, 481

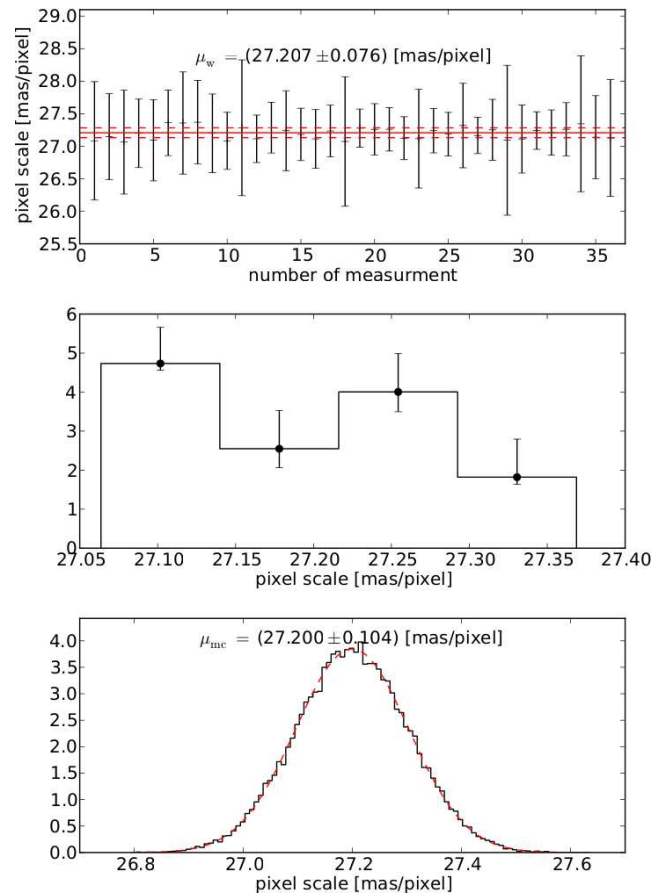


Figure A1. self-calibration result; pixel scale for 2008/02/15

APPENDIX A: PLOTS

For completeness we show the results of self-calibration for pixel scale and detector orientation for all epochs with same remarks as Fig. 3.

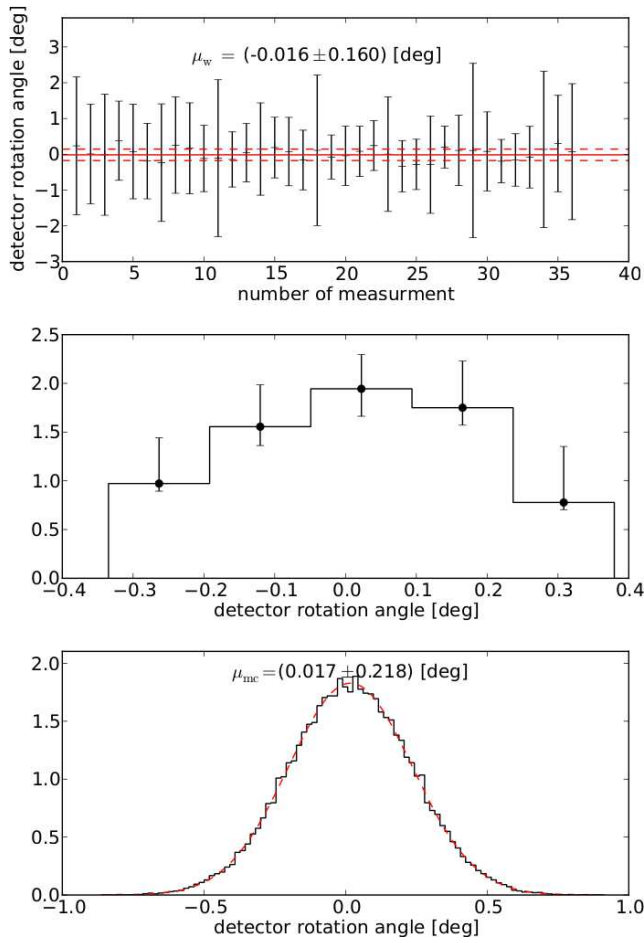


Figure A2. self-calibration result; detector orientation for 2008/02/15

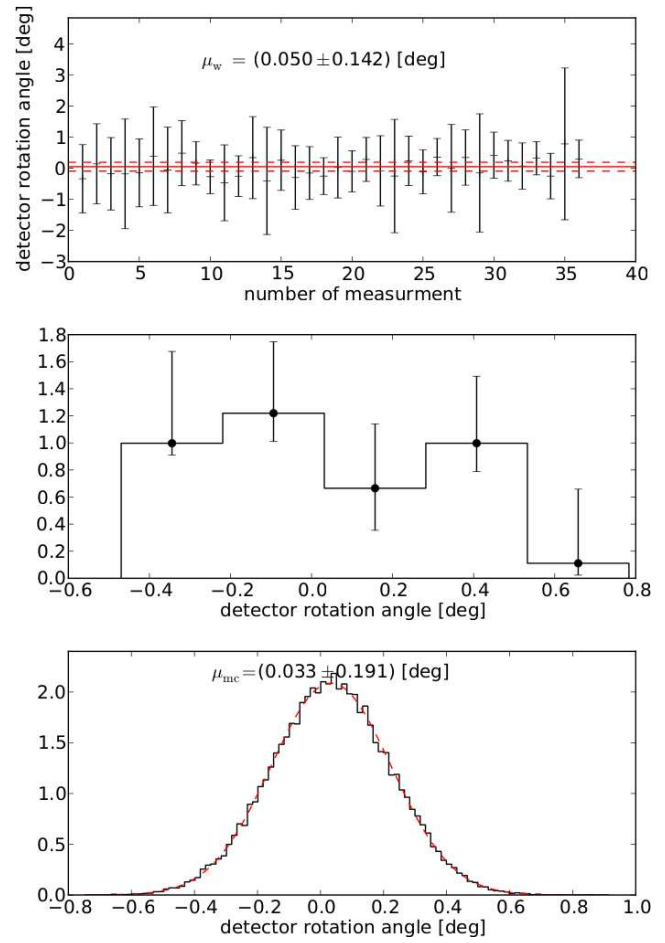


Figure A3. self-calibration result; detector orientation for 2004/12/16

APPENDIX B: TABLES

Table B1. Kinematic Parameter for Members of selected Cluster for UVW space velocity

Group	HIP	R.A. (J2000.0) deg	Dec. (J2000.0) deg	π mas	μ_α mas yr ⁻¹	μ_δ mas yr ⁻¹	RV km s ⁻¹	Reference for RV
Platais 9	44816	136.999	-43.433	5.99±0.11	-23.4±0.70	14.4±0.7	17.6±0.3	1
	45189	138.127	-43.613	4.71±0.46	-22.72±0.48	12.87±0.38	15.4±3.7	2
	45270	138.394	-47.338	6.40±0.25	-25.23±0.25	14.24±0.23	15.0±1.1	1
	45314	138.534	-44.146	6.20±0.27	-24.90±0.26	13.13±0.19	20.0±2.9	1
	45344	138.602	-43.228	5.33±0.26	-23.6±0.9	8.7±0.9	15.0±4.2	1
	45395	138.766	-48.504	5.00±0.63	-22.43±0.56	13.17±0.51		
	45820	140.138	-44.283	4.74±0.56	-24.2±1.0	13.8±1.1		
	46024	140.796	-44.965	5.54±0.48	-25.36±0.43	13.58±0.36		
Trumpler 10	42939	131.293	-41.427	2.22±0.86	-12.89±0.59	7.17±0.66		
	43055	131.574	-42.759	2.54±0.75	-11.99±0.57	7.00±0.58		
	43087	131.643	-42.791	3.09±0.95	-12.34±0.67	8.20±0.71		
	43128	131.772	-45.075	2.81±0.33	-12.85±0.30	6.34±0.25	32.0±4.5	1
	43182	131.95	-42.273	2.82±0.49	-12.86±0.37	6.13±0.40		
	43209	132.037	-42.463	2.07±0.30	-12.50±0.27	6.22±0.24	30.0±4.5	1
	43285	132.264	-43.761	2.63±0.53	-12.04±0.50	7.68±0.41	20.0±7.4	2
	43520	132.959	-44.151	1.94±0.33	-12.75±0.34	5.93±0.25	22.0±3.5	1
IC 2391	41644	127.374	-54.212	4.47±0.28	-16.6±1.0	17.7±1.0	10.1±4.0	3
	42121	128.792	-54.206	4.12±0.33	-14.72±0.32	15.77±0.34	10.0±7.4	2
	42216	129.098	-53.037	4.10±1.19	-15.8±1.3	25.7±1.3	22.0±7.4	2
	42274	129.294	-53.259	6.46±0.57	-24.96±0.55	23.0±0.5	6.0±7.4	2
	42374	129.6	-53.722	7.06±0.43	-23.72±0.46	22.00±0.42	21.0±7.4	2
	42400	129.687	-53.09	6.23±0.33	-25.53±0.36	21.84±0.3	11.7±3.5	1
	42450	129.819	-52.314	5.55±0.69	-24.69±0.65	22.41±0.57	12±999	4
	42459	129.849	-53.44	7.33±0.24	-23.90±0.24	23.46±0.22	15.0±4.2	1
	42504	129.99	-53.055	7.37±0.34	-25.5±1.2	20.8±1.0	14.5±1.2	5
	42535	130.073	-53.015	6.79±0.26	-25.30±0.27	23.14±0.24	14.6±4.3	1
	42536	130.073	-52.922	6.61±0.35	-25.1±0.9	25.0±0.9	16.1±0.7	1
	42702	130.542	-52.968	6.06±0.43	-25.60±0.46	23.23±0.42	-2.6±4.4	1
	42714	130.576	-53.902	7.81±0.94	-25.05±0.95	23.22±0.87	12.0±7.4	2
	42715	130.579	-53.1	6.53±0.26	-21.8±1.2	24.3±1.1	16.8±1.78	2
	42726	130.606	-53.114	6.73±0.17	-24.84±0.18	23.23±0.18	15.6±0.2	5
	42809	130.842	-52.209	2.83±0.68	-23.92±0.60	22.00±0.55		
	42823	130.887	-52.004	6.90±0.59	-27.57±0.52	26.32±0.50		
	43071	131.597	-52.844	5.25±0.51	-21.5±1.6	22.5±1.4		
	43195	132.001	-52.85	7.05±0.24	-25.10±0.25	23.31±0.25	11.6±1.5	1
	43433	132.696	-54.113	5.75±0.58	-23.1±2.2	19.6±1.8		

Note. Kinematic data for Cluster member stars according to Anderson & Francis (2012) with radial velocities from 1: Gontcharov (2006), 2: Kharchenko et al. (2007), 3: Levato et al. (1996), 4: Turon et al. (1993) and 5: Pourbaix et al. (2004).